Seismic actions on structures in the near-source region of the 2016 central Italy sequence

Iunio Iervolino,[1] Georgios Baltzopoulos,[2] Eugenio Chioccarelli,[2,3] Akiko Suzuki.[1]

Abstract. The central Italy seismic sequence began in the latter half of 2016 and continued well into 2017, causing severe damage in the villages close to the source and causing hundreds of casualties. It is a sequence especially interesting to study, from the perspective of seismic actions experienced by structures, because it saw nine M≥5.0 earthquakes within a period of five months, rupturing parts of the complex central Apennine mountain range fault system. Consequently, some of the main earthquake engineering issues that arose are the multiple locations where the code-mandated seismic actions were exceeded in more than one of the main events of the sequence and the number of pre- and low-code existing buildings that suffered heavy damage or collapse due to the intensity of individual earthquakes and the cumulative effect of repeated damaging shocks. The present article picks up on these topics and uses probabilistic seismic hazard, as well as the multitude of strong ground motion recordings available from the sequence, to provide a discussion on certain issues, that are all related to the topical subject of seismic actions. These issues are: (i) the unsurprising exceedance of code spectra in the epicentral areas of strong earthquakes; (ii) the particular spectral shape and damaging potential of near-source, pulse-like, ground motions, possibly related to rupture directivity; and (iii) structural non-linear behaviour in the wake of a sequence that produces repeated strong shaking without the necessary respite for repair and retrofit operations.

1. Introduction

Since the end of August 2016, an extended region of central Italy has experienced a long lasting seismic sequence (Luzi et al., 2017). The initiating event was the Amatrice earthquake that occurred on August 24th, 2016 at 1:36:32 UTC. The event was characterized by a moment magnitude (M) equal to 6.0 and heavily damaged the villages of Amatrice and Accumoli. It caused about three-hundred fatalities, resulting from the collapse of several buildings in the area closest to the source. During the coming months, and until June 2017, nine seismic events surpassing M5.0 occurred in the area. Notable among these were two events that occurred on October 26th, one at 17:10:36 UTC (M5.4, epicenter near the village of Castel Sant'Angelo sul Nera) and another at 19:18:06 UTC (M5.9 near Ussita). The largest event of the sequence (M6.5) occurred on October 30th at 06:40:18 UTC with the epicenter located in the vicinity of the town of Norcia;[4] this event will be hereafter identified as the mainshock of the sequence. The sequence continued into 2017, with four more events with M between 5.0 and 5.4 occurring on the same day, January 18th, in the area between the villages of Amatrice and Pizzoli. In Figure 1 the sequence is represented in terms of number of earthquakes with magnitude larger than 2 in cells 5km by 5km wide and the corresponding released cumulative seismic moment, from the beginning of the sequence up to February 2017.

This long-duration seismic sequence came in the wake of the 2009 L'Aquila earthquake and the 2012 Emilia sequence to rekindle scientific debate on, among other topics, the seismic actions considered for structural design (regarding the earlier events see also Chioccarelli and Iervolino,

Corresponding author: iunio.iervolino@unina.it

[1] Dipartimento di Strutture per l'Ingegneria e l'Architettura, Università degli Studi di Napoli Federico II, Italy.

[2] Istituto per le Tecnologie della Costruzione, Consiglio Nazionale delle Ricerche (ITC-CNR), Italy.

[3] Università Telematica Pegaso, Italy.

[4] Ground motion data and source information about on these events can be found at http://esm.mi.ingv.it/, via the following *Event ID* codes: EMSC-20160824_0000006 (Amatrice M6.0), EMSC-20161026_0000095 (Ussita M5.9), EMSC-20161026_0000077 (Castelstantagelo sul Nera M5.4), EMSC-20161030_0000029 (Norcia M6.5).

2010; Iervolino et al., 2012b). In fact, during this central Italy sequence, many communities found themselves near the source of different seismic events, sustaining considerable damage, especially to old constructions, not built according to current standards or even to any seismic provision at all. What is more, several settlements were found in that near-source situation more than once. In those cases, the extent of the damage suffered by the building stock was, at least partly, attributable to the cumulative effect of being subjected to repeated strong motion shocks and the peculiar features of shaking close to the seismic rupture.

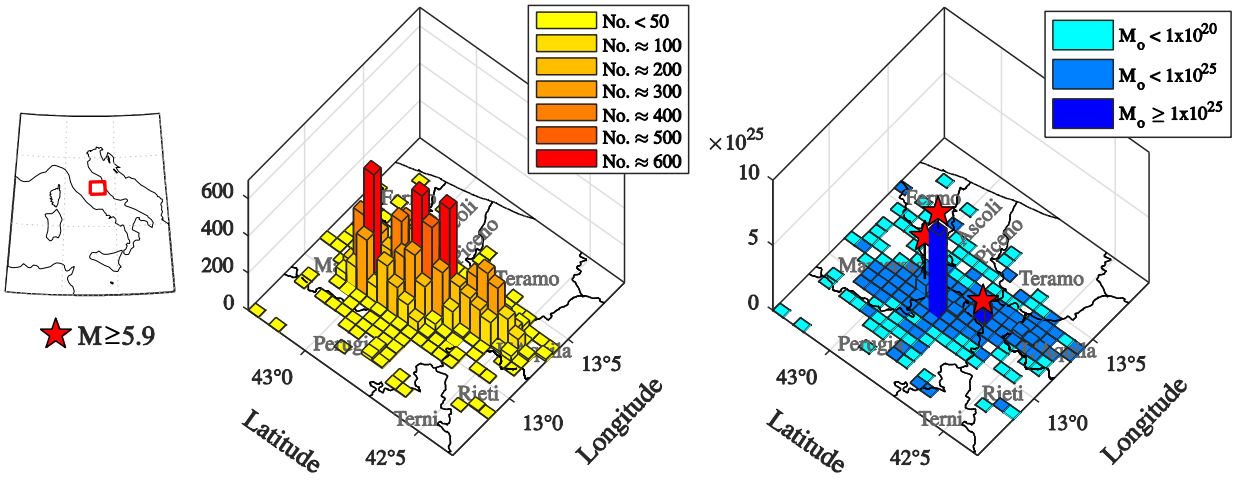

Figure 1. Number of earthquakes with M≥2 recorded in 5km by 5km cells during the Aug. 24th 2016 – Feb. 24th 2017 period (left) and corresponding released cumulative seismic moment: M_0 [dyne×cm] (right). Data from http://cnt.rm.ingv.it/, last accessed February 2017.

From a scientific, earthquake engineering and engineering seismology, point of view this sequence is unique in the Italian history of instrumental seismicity so far. This is because of the number of large earthquakes recorded in a relatively short time, and the acquisition of about ten-thousand recorded ground motions which have been made available by the Italian Accelerometric Network (RAN, *Presidency of the Council of Ministers*, 1972; http://ran.protezionecivile.it/), managed by the *Department of Civil Protection* (DPC), and the Italian seismic network (RSN), managed by the *Istituto Nazionale di Geofisica e Vulcanologia* or INGV (INGV Seismological Data Centre, 1997; http://cnt.rm.ingv.it/instruments/network/IV). Furthermore, the progressively increasing density of a temporary accelerometric network that was deployed as the sequence unfolded meant that a large number of near-source ground motions were recorded.

This bulk of near-source ground motions forms the base material for the present study, by virtue of being the most significant part of the overall recordings from a structural point of view. The ensuing discussion focuses on three specific issues generally pertaining to the topic of seismic actions for seismic design and assessment, addressing them in light of the specific features of such a strong sequence. In the following, attention is first given to the fact that the pseudo-acceleration spectra (or simply acceleration spectra from here on) of ground motions recorded in areas close to the seismic sources of the strongest events of the sequence, exceeded the design actions provided by the national code for new constructions. Then, the identification of near-source pulse-like records in the sequence and their effect on simplified structural response is addressed; this is a topical issue, which is still not explicitly or appropriately accounted for by even state-of-the art seismic codes (the Italian code included). Finally, the damage accumulation effect due to repeated seismic shocks is analysed for some locations that have been subjected to at least five structurally damaging shakings.

2. Should code spectra be questioned because they are exceeded close to the source?

During the central Italy sequence, elastic spectra at the basis of design of ordinary constructions in Italy have been systematically exceeded, in areas relatively close to the seismic source, by recordings of more than one earthquake. To picture this observation, the maps in Figure 2 report the source surface projections (dashed lines) for the three main events as well as the locations of the stations (depicted as triangles) which have recorded these earthquakes in an area of about 8800 km^2. Black triangles indicate locations where the code spectra for life-safety limit state design of ordinary new constructions in the most recent Italian seismic code (C.S.LL.PP. 2008, NTC hereafter) have been exceeded at least in one spectral ordinate in the range 0s-2s and for at least one of the two horizontal recording directions: east-west (EW) and north-south (NS).

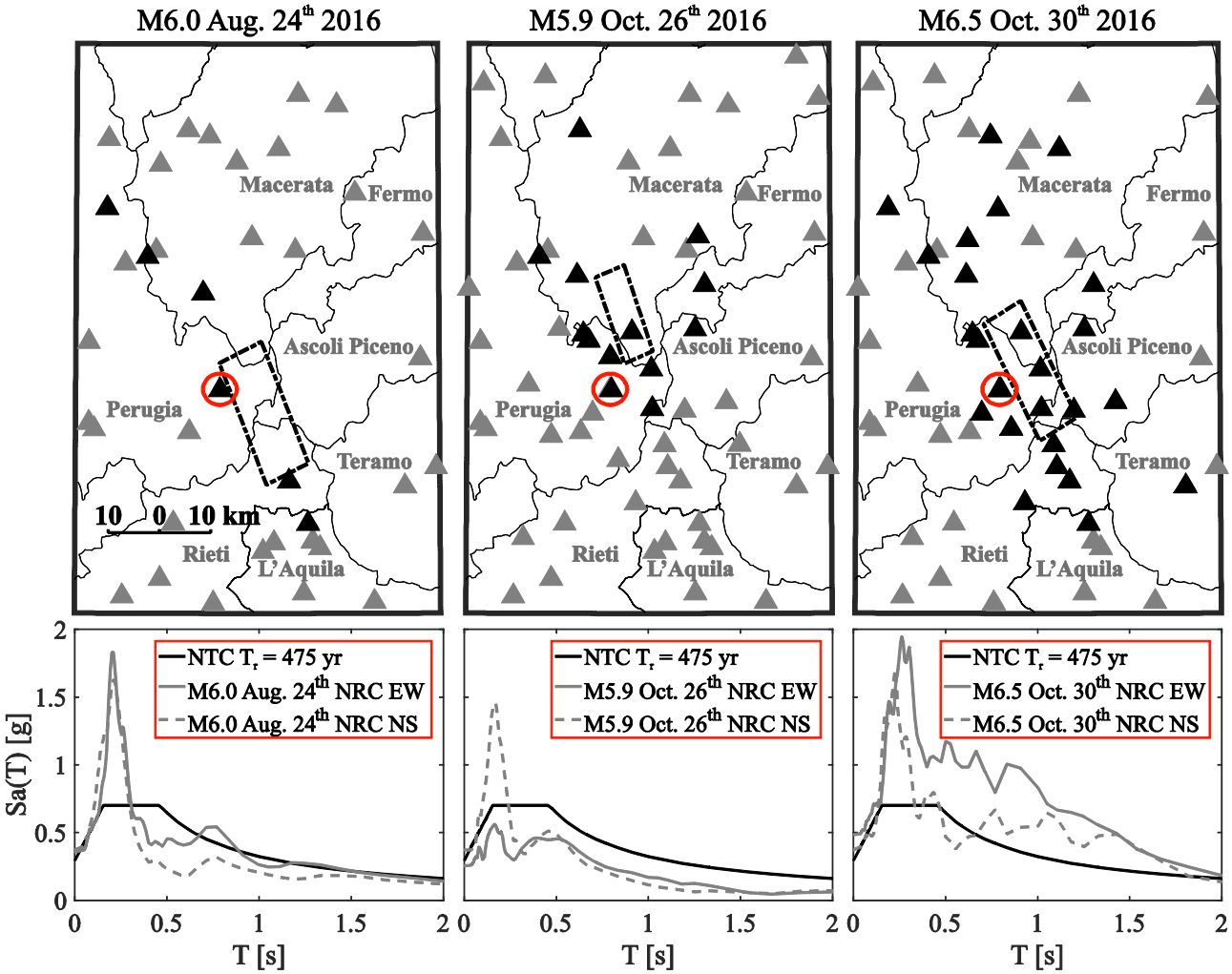

Figure 2. Top: maps of stations recording the main events of the sequence. Black triangles are the stations where horizontal code spectra were exceeded at least in one ordinate between 0s and 2s. Bottom: code and recorded spectra at NRC station (Norcia). Left column Aug. 24th 2016 M6.0, center column Oct. 26th 2016 M5.9, right column Oct. 30th 2016 M6.5.

It is apparent that code spectra have been systematically exceeded and this raised a question that has been also asked due to similar observations in preceding events in Italy, such as the 2009 L'Aquila earthquake and the 2012 Emilia sequence (see, for example, Akinci et al., 2010 and Meletti et al., 2012): are code spectra underestimated as we see systematic exceedance in major seismic events? The rest of this section demonstrates that exceedance of code spectra close to the source is quite

expected by the very definition of code spectra and, as a consequence, underestimation of design seismic actions cannot be claimed based on these observations alone.

Code spectra in Italy are based on probabilistic seismic hazard analysis (PSHA). PSHA allows one to compute the rate (λ_{im}) of earthquakes exceeding a given ground motion intensity measure (IM) threshold (im) at a site of interest (McGuire, 2004), Equation (1). In the equation, *n* is the number of seismic sources relevant for the hazard at the site, ν_i is the annual rate of earthquake occurrence on source *i*, $f_{M,R}(m,r)$ is the joint probability density function of magnitude and source-to-site distance (R) and, finally, $P[\mathrm{IM} > im|m,r]$ is the probability of exceeding the intensity measure threshold. The latter probability is provided by a ground motion prediction equation (GMPE).

$$\lambda_{im} = \sum_{i=1}^{n} \nu_i \cdot \int_M \int_R P[\mathrm{IM} > im|m,r] \cdot f_{M,R}(m,r) \cdot dm \cdot dr \qquad (1)$$

If the IM is the elastic spectral pseudo-acceleration (Sa) at different natural oscillation periods (T), it is possible to build the *uniform hazard spectrum* (UHS). All the ordinates of the UHS are characterized by the same exceedance rate or, equivalently, are exceeded once every so many years on average; i.e., their exceedance has the *same return period* (T_r). According to the NTC, design elastic response spectra are close approximations of UHS' determined via the study described in Stucchi et al. (2011), which computed uniform hazard spectra over a grid of more than 10,000 points for 9 return periods from 30 years to 2475 years (http://esse1.mi.ingv.it/, last access July 2017) all-over the country, considering rock site conditions.

At this point, more details on Figure 2 can be given. In NTC, the return period of the spectrum to be used in design or assessment depends on the limit-state considered and on a reference period proportional to the design life of the structure in question. For ordinary (e.g., residential or office) constructions, the return period of the code spectrum for the life-safety limit state is 475yr. Figure 2 refers to the exceedance of at least one spectral ordinate in the range 0s-2s of such spectra in the area of the sequence. Code spectra were adjusted for local site conditions according to the prescription of the code and the geological information of the recording sites retrieved by the Engineering Strong Motion database (ESM, http://esm.mi.ingv.it, last access July 2017). To provide a more quantitative measure of the issues, Table 1 counts the number of exceeding stations and the corresponding percentage with respect to the total number of stations recording the events for bins of distance from the source. The metric used for distance is the minimum distance from the surface projection of the source that is usually termed Joyner and Boore (1981) distance (R_{jb}). As shown, all stations within 10km from the source exceeded life safety design actions during both the M6.0 and M6.5 events, while 78% did so during the M5.9 event. As expected, these percentages rapidly decrease with increasing distance: 20%, 37% and 62% of the stations within 30km from the source exceeded design actions during the M6.0, M5.9 and M6.5 events, respectively.

Red circles in the maps of Figure 2 identify one of the two stations that exceeded code spectra in all the three considered events; one such of stations is Norcia (NRC) while the other, not considered in the following, is FOC (Foligno Colfiorito, located on the boundaries between Macerata and Perugia provinces). For each event, recorded NRC response spectra are reported in the figure below the

corresponding map, along with the $T_r = 475\text{yr}$ code spectrum for the same site. The exceedance in the range of periods of about 0s-0.25s is common to the three events.[5]

Table 1. Statistics of $T_r = 475yr$ code spectra exceedance per bin of distance from the sources.

	M6.0 – August 24th 2016		M5.9 – October 26th 2016		M6.5 – October 30th 2016	
R_{jb}	No. Exceedances	No. Exceedance /No. Stations	No. Exceedances	No. Exceedance /No. Stations	No. Exceedances	No. Exceedance /No. Stations
<10	2	100%	7	78%	14	100%
<20	4	36%	12	50%	22	79%
<30	5	20%	13	37%	23	62%

The observed exceedances of design actions triggered a scientific debate about the possible inadequacy of the hazard assessments derived from PSHA. It has been discussed elsewhere (e.g., Iervolino, 2013), that data acquired in the epicentral area of a single event cannot be sufficient to substantiate an alleged underestimation of code spectra derived from hazard analysis. This is because a time-span of many years is necessary to validate the frequency associated with exceedance of a certain ground-motion intensity at a site.[6] Conversely, it is well expected by the nature of code spectra that they are exceeded in the epicentral area of relatively high-magnitude earthquakes, even if these earthquakes are fully considered by the hazard analysis used to build the spectra. In fact, PSHA, in assessing seismic hazard for a specific site, accounts for ground motions from all possible earthquake locations and magnitudes (building a spectrum which does not represent a specific event). Because ground motion intensity (at least when spectral acceleration is concerned) tends to decay with distance from the source, the greatest effects of any given event are necessarily observed close to the source. In other words, in the case of large seismogenic zones, as those of the model by Meletti et al. (2008) that were used to build code spectra in Italy, significant contributions to probabilistic seismic hazard are almost exclusively due to possible earthquake locations closest to the site (exception to this statement may occur in specific cases when multiple zones are concerned; see Iervolino et al., 2011). Moreover, the more frequent earthquakes among those considered in PSHA are, typically, those with comparatively lower magnitude; conversely, the largest magnitude events are relatively rare. It follows that, given a UHS for a medium-long return period (say, for example 475yr), its ordinates are unlikely to be exceeded by an earthquake that occurs at the site quite frequently, while they are very likely going to be surpassed in the case of an earthquake with rare magnitude occurring close to the site.

To substantiate this discussion, in the following figures it is quantitatively illustrated that such exceedances should have been well expected within the areas close to the seismic sources. To this aim, one should first recall that the PSHA behind the NTC spectra was performed via a logic tree comprising 16 branches. The results of "branch 921" are claimed to be the closest to the hazard estimate provided by the full logic tree (Stucchi et al., 2011). This branch considers the ground motion

[5] Although there are several recording stations outside the boundaries of the maps, none of them has exceeded the life-safety code spectrum for ordinary structures. Exceptions are the stations AQK (L'Aquila) and MMUR (Monte Murano). AQK experienced exceedances during the M6.0 and M6.5 events, being distant from the source 34km and 43km, respectively. These exceedances are due to the unusual shape of recorded ground motions with increment of spectral ordinates in a narrow range of periods around 1.5s, probably due to local effects that have been discussed, among others, in Monaco et al. (2009). Exceedance at MMUR occurred during the M5.9 event at 49km distance. Exceedance is slight (i.e., recorded spectrum is 5% higher than code's) at 0.1s vibration period.

[6] One may argue that multiple exceedances have been observed in this sequence, yet it should be recalled that PSHA, and therefore code spectra in Italy, refer to exceedance due to mainshocks only and does not account for exceedances caused by aftershocks or foreshocks to the main event of the sequence.

prediction equation (GMPE) of Ambraseys et al. (1996) and the style-of-faulting correction factors proposed by Bommer et al. (2003). These models are also considered herein for consistency. It is also worth recalling that the seismogenic source model at the basis of PSHA used to develop NTC spectra considers maximum magnitude larger than 7 for the zone where the central Italy sequence occurred, thus observed magnitudes are accounted for by code spectra.

In order to identify the areas in which the exceedance of design seismic actions should have been expected upon occurrence of the events considered in Figure 2, one has to consult Figure 3. In the figure, the surface projection of the ruptures and the provinces' administrative boundaries are shown. The background colours of the maps represent, for each site, the values of code spectra with 475yr return period (on rock). For representation needs, two spectral ordinates are considered, peak ground acceleration (PGA) and $Sa(1\text{s})$, both indicated as $im_{475\text{yr}}$. Their values are from http://esse1.mi.ingv.it/d2.html (last accessed in May 2017). Solid lines are the contours of the exceedance probability (p) of $im_{475\text{yr}}$, which are drawn plugging in the GMPE of Ambraseys et al. (1996) the actual magnitude of each event and considering, for each site in the map, the actual distance from the source surface projection, Equation (2). With this information, the GMPE provides the probability that the considered code spectra ordinates are exceeded by an event of the kind as each of those occurred.

$$p = P\left[\text{IM} > im_{475\text{yr}} \middle| m, r_{jb}\right] \tag{2}$$

For the three considered events, when PGA is of concern, the probabilities of exceeding design actions are large: maximum exceedance probability is 0.76, 0.77 and 0.90 for the M6.0, M5.9 and M6.5 event, respectively. This means that it was almost certain that design PGA were going to be exceeded at sites close to the rupture. Such exceedance probabilities rapidly decrease when the source-to-site distance increases. On the other hand, when $Sa(1\text{s})$ is the selected IM, maximum exceedance probability is 0.78 in the case of M6.5 while, for the M6.0 and M5.9 events, maximum probabilities are 0.48 and 0.46, respectively.

These calculations confirm the initial premise of this section, that the high likelihood of exceeding code spectral ordinates close to the source of earthquakes of this magnitude is nothing unexpected and does not warrant surprise.

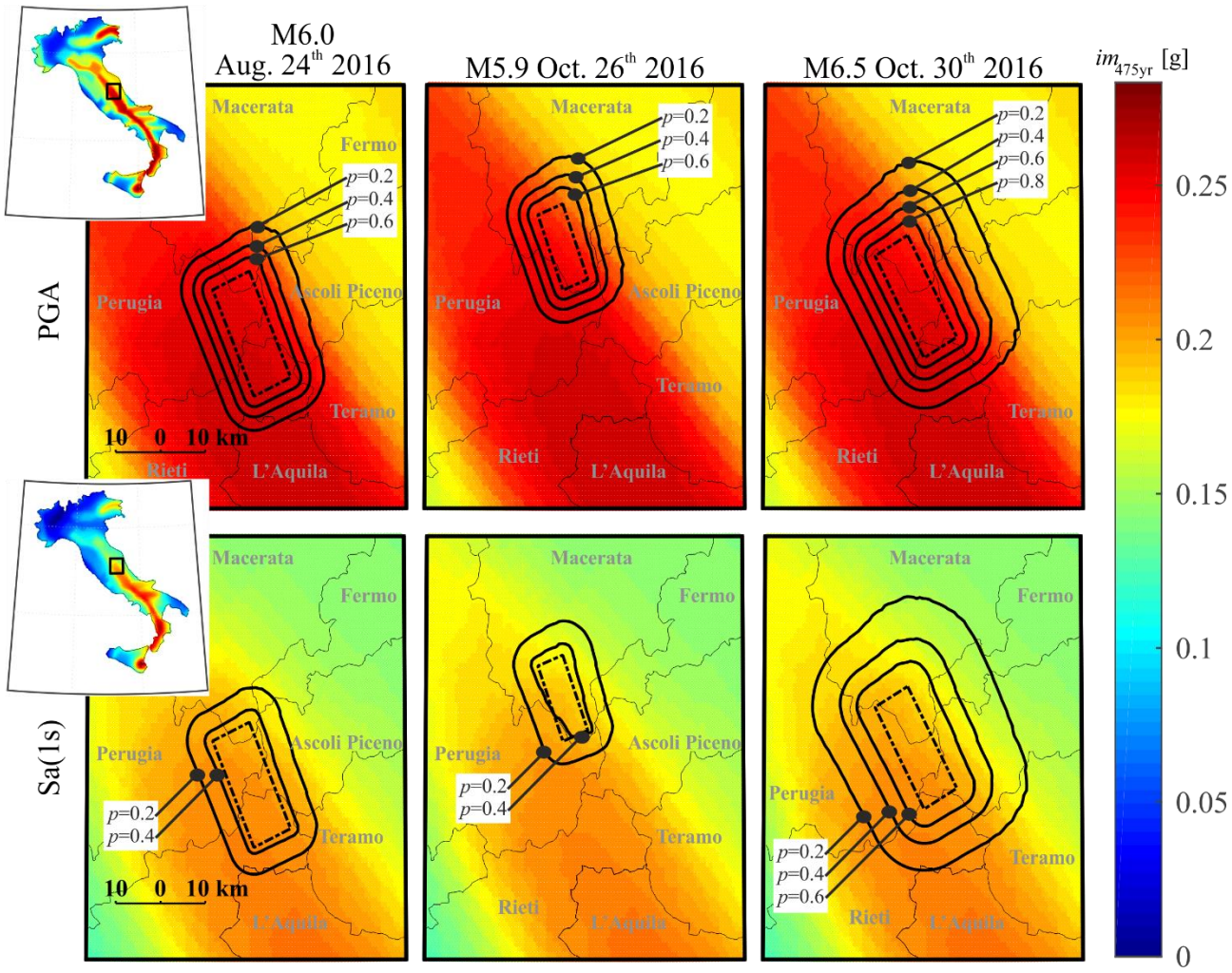

Figure 3. Probability of exceedance of NTC design actions for $T_r = 475\text{yr}$ in the near-source areas of the three main events of the sequence - top: PGA; bottom: $Sa(1\text{s})$. Left column: Aug. 24th 2016 M6.0; center column: Oct. 26th 2016 M5.9; right column: Oct. 30th 2016 M6.5. (Upper-left corner panels are nationwide maps of $im_{475\text{yr}}$.)

3. Pulse-like vs ordinary records: spectral shape and inelastic response

As discussed in the previous section, the exceedance of code spectra in near-source areas does not constitute, per se, a proof of flawed derivation of the spectra. However, it is well known that ground motion in near-source regions is affected by systematic spatial variability that, for a number of reasons, is neither captured nor appropriately represented by classical PSHA. Pulse-like records constitute one of the manifestations of such spatial variability. Impulsive features in ground motions have been identified in earthquakes since quite some time, yet have been relatively less studied in the case of normal-faulting earthquakes (Chioccarelli and Iervolino, 2010), which constitute the dominant focal mechanism in the area of the central Italy seismic sequence.

Near-source, pulse-like, ground motions constitute a special category of seismic input, whose engineering relevance has been long recognized (Bertero et al., 1978). The most prominent causal mechanism of impulsive ground motion is rupture directivity: at sites located along the propagation direction of shear dislocation on the fault, shear wave fronts emitted at distinct times may arrive almost simultaneously. This can lead to a constructive wave interference effect, observable on the ground velocity trace as a coherent, double-sided pulse that caries most of the seismic energy (Somerville et al., 1997). A consequence of this feature is that such ground motions, on average, can

subject ductile structures to greater inelastic displacements, with respect to non-impulsive seismic input (e.g., Iervolino et al., 2012a), thus attracting the research interest of earthquake engineers.

It is worth noting that the emergence of pulse-like ground motions is never guaranteed at all near-source sites and that the probability of observing them depends, among other factors, on site-to-source geometry and focal mechanism (Iervolino and Cornell, 2008; Iervolino et al., 2016a). This nuance partly explains the relative scarcity of pulse-like records found in ground motion databases in the past, as it is hard to capture this phenomenon without a dense accelerometric network spanning the epicentral area. In recent years, seismic events nucleating in the vicinity of denser, modern seismic networks (e.g., Parkfield, California, 2004; L'Aquila, Italy, 2009) have provided more empirical evidence in terms of impulsive recordings, further spurring research into the topic. In this respect, the central Italy sequence of 2016 stands out for having provided a significant number of high quality, near-source ground motion recordings, thanks to the multitude of temporary accelerometric stations deployed to closely monitor seismic activity, following the August 24th 2016, M6.0 initiating event.

In Luzi et al. (2017), these near-source records were investigated for pulse-like characteristics using the continuous wavelet transform algorithm proposed by Baker (2007). As a side-note, it should be underlined that such methods of identifying pulse-like characteristics in recorded ground motion rely on data that is tractable directly and exclusively from the velocity time-history. For this reason, rupture directivity can be considered a likely causal mechanism of such features but in the absence of direct links with the physical process of fault dislocation, a verdict in that direction cannot be reached with certainty. Having made this premise, that operation resulted in a set of eighteen ground motions being identified as pulse-like. These ground motions were recorded during three of the events comprising the 2016 sequence, namely the August 24th M6.0 shock, the October 26th M5.4 shock and the October 30th M6.5 (main)shock. Figure 4 shows maps of the positioning of accelerometric stations around the rupture plane's horizontal projection of the 24th Aug. and the 30th Oct. 2016 events, with distinction made among those that recorded pulse-like and non-pulse-like (i.e., ordinary) motions. The increase in network density during the time interval between the two events is evident. The same figure shows the most prominent impulsive velocity traces identified, as well as the velocity traces of some nearby ordinary recordings (fault-normal, FN, component) for comparison. The orientation of each impulsive components depicted is indicated on the maps (this information is also available on http://esm.mi.ingv.it).

This ground motion set is used in the present article to discuss the differences between pulse-like and *ordinary* (i.e., non-impulsive) records in terms of spectral shape and structural seismic demand, the two being closely related as the former can have important influence on the latter (e.g., Baker and Cornell, 2005). For the benefit of this comparison, a set of ordinary ground motions is also assembled, from within those recorded during the 2016 seismic sequence. Thus, the ordinary set contains sixty-two ground motions recorded at sites with subsoil classified as A, B or C according to NTC (avoiding known soft soil sites), exhibiting PGA in excess of 0.10g and belonging to the four highest moment magnitude events of the 2016 sequence.

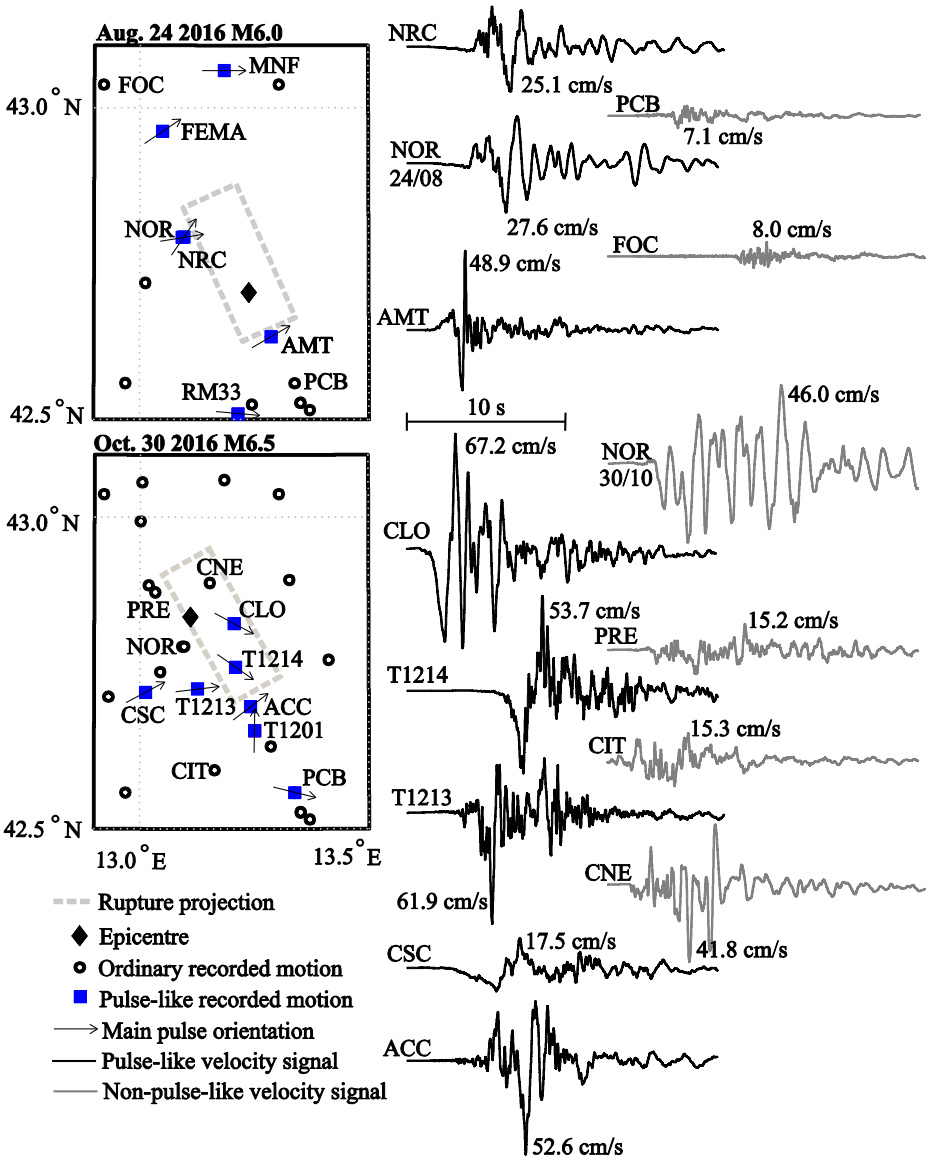

Figure 4. Position of accelerometric stations that recorded pulse-like or non-pulse-like ground motions (according to Luzi et al., 2017) relative to the horizontal projection of the rupture plane, for the 24th Aug. 2016 M6.0 and 30th Oct. 2016 M6.5 events. Velocity traces of pulse-like (black lines) and non-pulse-like (grey lines) records shown for comparison (station codes reported close to the signals); amplitude scale and duration (twenty seconds) is common to all depicted velocity time-histories. Orientation of pulse-like components is shown on the maps; non-pulse-like components are always shown in the fault-normal (i.e., strike-normal) direction.

A well-documented fact, regarding the response spectra of pulse-like ground motions, is the dominant role of the impulsive waveform in the determination of the spectral shape in terms of pseudo-velocity. An example of this effect is provided in Figure 5, where the velocity trace of the impulsive horizontal component is shown for the recording obtained at station CLO (Castelluccio di Norcia), along with the impulsive waveform extracted by the identification algorithm. The pseudo-spectral velocity (PSV) of this impulsive signal is plotted in Figure 5 (right) against PSV due to the extracted pulse alone; one notes the broad peaks appearing around a period equal to the pulse period (or pulse duration) T_P.[7]

[7] In fact, the vibration period for which PSV attains its maximum value has been used in the past as a proxy for T_P.

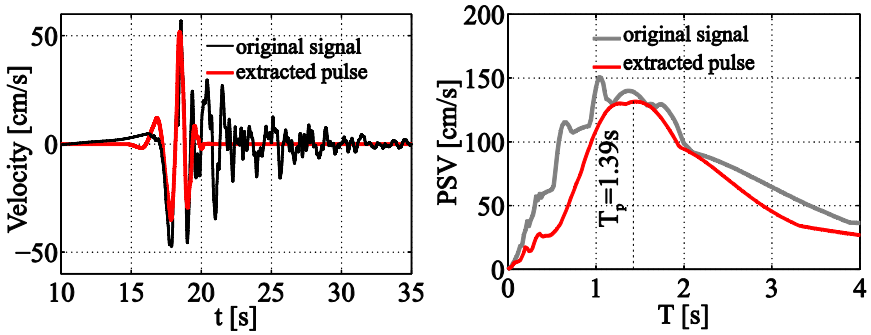

Figure 5. Velocity time history and extracted pulse (left) and corresponding pseudo-spectral velocity (right) for the CLO (Castelluccio di Norcia) record of the October 30th 2016 M6.5 shock.

The imprint of the pulse can also be found on the pseudo-acceleration spectrum, even if it is less pronounced than in terms of PSV. While Somerville et al. (1997) initially suggested a broadband amplification model to account for the emergence of pulses on Sa GMPEs, modern consensus has gradually shifted towards narrowband amplification schemes centered around T_P (e.g., Shahi and Baker, 2011). Put in different words, for a given magnitude of causal event, site-to-rupture distance and site conditions, larger-than-average Sa ordinates are expected for pulse-like horizontal ground motion components than for ordinary ones, at least for periods around the vicinity of T_P. Typically, when observing the effect of this narrowband amplification on average spectral shape over a large set of pulse-like motions, the result appears broadband. This is due to the variability that T_P tends to exhibit even within a single event and can be observed here as well, since the sequence provided enough pulse-like records for considerations on average spectral shape to be meaningful. Spectral shape can be represented by normalizing the Sa ordinates of various records by dividing with the corresponding PGA and plotting the resulting spectral amplification factor Sa/PGA against vibration period. This normalizing operation was performed for the pulse-like and ordinary records mentioned earlier and the results are presented in Figure 6. It should be noted that, the majority of pulse-like records identified within the sequence by Luzi et al. (2017) exhibited prominent pulses around the FN orientation (see also Figure 4). In fact, this is the direction where directivity-induced pulses are mostly expected, due to the polarization of shear wave radiation patterns.

Figure 6 (left) offers a comparison of the average spectral shape of the pulse-like horizontal components with the spectral shape of the geometric mean (geomean for short) of the ordinary recordings' horizontal components. It can be observed that at high frequencies (up to a period of around 0.20s) ordinary ground motions, on average, slightly supersede the impulsive ones in terms of spectral amplification factors. On the other hand, a wide spectral region from 0.40s to 3.0s sees clear predominance of the pulse-like set's average amplification over the geometric mean of ordinary ground motions. This is actually the period range where the detected pulse periods were found, rendering this result consistent with previous observations.

An analogous, but less pronounced, difference is observed in Figure 6 (right) between the average spectral shape of the pulse-like components and the corresponding average of the transverse components of the same pulse-like records (which, in the vast majority of cases, are not considered impulsive). Although not shown here, it was observed that average spectral shapes of the FN and fault-parallel (FP) rotated ordinary components are, by contrast and as expected, quite similar with each other.

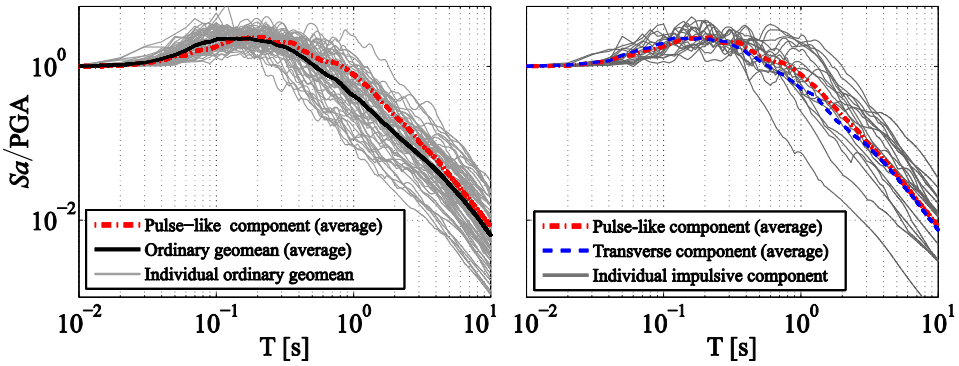

Figure 6. Left: Spectral amplification factors (individual and average) of the ordinary ground motion set compared with the average of the pulse-like horizontal components. The ordinary set comprises all non-pulse like ground motions recorded during the sequence with PGA>0.10g on stiff-to-firm soil or rock and the geomean of horizontal components is used. Right: spectral amplification factors of the impulsive horizontal components (individual and average) compared with the average of the transverse components of the pulse-like set

Previous research has suggested that this systematic difference in spectral shape between pulse-like and ordinary records (affected by T_P) is directly related to the larger average seismic demand imposed on structures by the former when compared to that of the latter (Tothong and Cornell, 2008; Bojórquez and Iervolino, 2011). In the present study, the aspect of inelastic seismic response to pulse-like vs. ordinary records is investigated via incremental dynamic analysis (IDA, Vamvatsikos and Cornell, 2002) and comparison of the results with the analytical model of Baltzopoulos et al. (2016) is made. This investigation employs two example single-degree of freedom (SDOF) structures that have a common trilinear (elastic-hardening-softening branch) monotonic backbone and follow a peak-oriented hysteretic rule that undergoes moderate cyclic strength deterioration (for the implementation in OpenSEES software; see Altoonash and Deierlein, 2004). The two systems have periods of natural vibration of 0.50s and 1.00s and a yield force set at 20% and 12% of gravity loads, respectively. The hysteretic behavior of the $T = 0.50s$ structure can be seen in Figure 7, where the response of the system under cyclic load reversals is plotted in terms of ductility, μ, defined as the ratio of displacement to yield displacement, $\mu = \delta/\delta_y$. These SDOF systems can be regarded as pushover-based idealizations (e.g., Vamvatsikos and Cornell, 2005) of low-to-mid-rise, low-code structures, representative of some structures one might encounter in the zones damaged by the central Italy sequence.

IDA was performed using the eighteen pulse-like component set and both sixty-two ordinary component sets (FN and FP). For each single record, the spectral acceleration causing collapse of the structure was calculated, indicated as Sa^{col}, collapse being defined as reaching the point of zero lateral strength. This result for the pulse-like records, is plotted in Figure 7, against pulse period-to-vibration period ratio T_p/T.

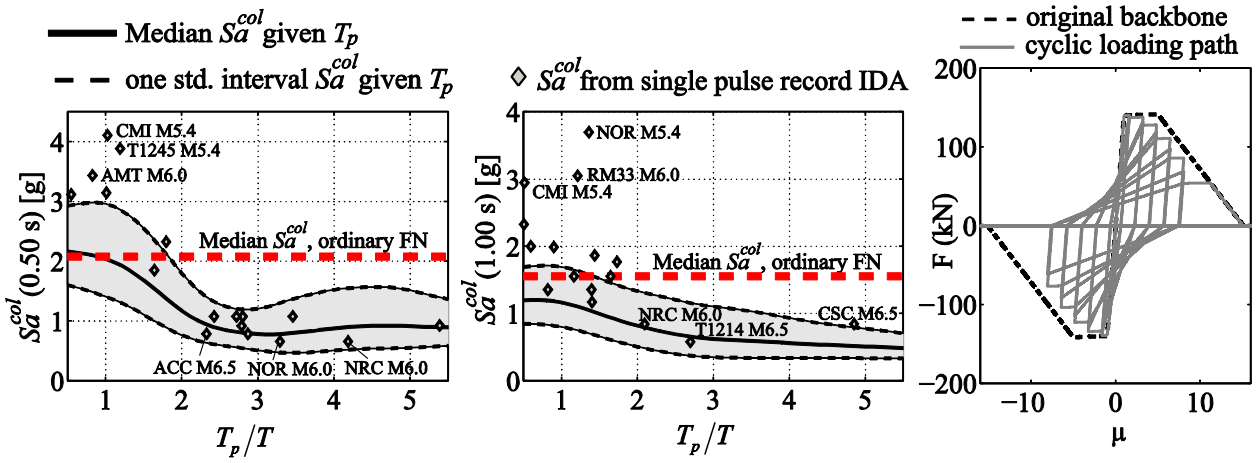

Figure 7. Collapse intensity of pulse-like records from the Central Italy sequence estimated via IDA, compared with collapse intensity given T_p according to the Baltzopoulos et al. (2016) for a SDOF structure with period $T = 0.50$s (left) and one with period $T = 1.00$s (center); trilinear backbone curve and hysteretic response to cyclic loading common to both SDOF structures used in the analysis (right).

For comparison reasons, two more results are reported on the same panel: the median Sa^{col} obtained from the ordinary ground motion FN component set (FP result omitted, being too similar to the FN one) and the analytical prediction provided for the same SDOF system by the model of Baltzopoulos et al. (2016). For the latter case, both median and plus/minus one standard deviation interval are shown (shaded area) assuming a lognormal distribution of Sa^{col} given impulsive seismic input with fixed T_P. In the literature, pulse-like records causing inelastic demand lower than the average of ordinary records (in Figure 7, those appearing above the red dashed line) are sometimes termed as *benign*, while those that cause higher demand are termed as *aggressive* records; this nomenclature is also used here.

It can be observed from Figure 7 that in the region defined by $T_p/T > 2$ (a region where previous studies have shown that impulsive input is typically more aggressive towards inelastic structures than ordinary seismic input) the central Italy sequence pulse-like records generally fall around the median prediction of the analytical model and never tread outside the shaded area that denotes one standard deviation distance from that median. Overall, in the case of $6 > T_p/T > 2$ both the analytical model and the numerical results from the sequence's impulsive input confirm the expected increased seismic demand with respect to the ordinary case: for the $T = 0.50$s system, the former provides Sa^{col} average values around 1.0g and the latter slightly above 2.0g while the corresponding situation for the $T = 1.00$s structure sees a comparison of around 0.85g (pulse-like) to 1.60g (ordinary). On the other hand, the shorter-period pulses clustered around $T_p/T = 1$ appear to exhibit a greater-than-average benign effect on this structure, as quantified by Sa^{col} values exceeding the median of the ordinary set as well as the median-plus-standard-deviation analytical predictions. Note that the most benign and most aggressive of ground motions are tagged in the plots by recording station, in order to reveal potentially systematic culprits of one behavior or the other.

Generally speaking, the sample of pulse-like motions provided by the central Italy sequence contained enough records to allow for some considerations in terms of average spectral shape and expected inelastic response. The discussed agreement with previous studies in these matters of engineering significance is important, since from an engineering seismology perspective, pulse-like motions nascent from normal faulting mechanisms used to be, as mentioned, a rarity in the databases and there

are hints in the literature suggesting that the underlying rupture-related mechanisms can differ from those associated with strike-slip events (Howard et al., 2005, Poiata et al., 2017).

4. Sequence effects on non-linear structural response

Structures designed according to modern seismic codes, are typically expected to cope with rare ground shaking intensities through dissipating seismic energy by sustaining a certain amount of damage. Seismic design according to these codes implies possible failure (i.e., exceedance of a limit state) due to a single event (which is not directly related but is coupled with the fact that classical PSHA only accounts for mainshocks). In fact, an underlying assumption of this concept, is that damaging events will not only be rare, but also enough far apart in time to allow for a damaged structure to be repaired in the meantime. This reasoning can clearly fall through in the case of seismic sequences. In fact, in recent years, the concept that structures damaged by a mainshock earthquake may be unable to meet performance criteria during the aftershock sequence that follows, due to deterioration of lateral force resisting mechanisms and seismic energy dissipation capacity, has been receiving increased attention in earthquake engineering research (e.g., Yeo and Cornell, 2009; Iervolino et al., 2016b). A conceptually similar, but less studied situation is the case at hand: a series of strong shocks, potentially damaging individually, closely clustered in time and space.

During the 2016 central Italy seismic sequence, within a course of less than ninety days, some sites repeatedly found themselves at close distances to ruptures corresponding to events of magnitude M≥4. The most notable such case is the town of Norcia, that was found at epicentral distances of 15km or less during events with $M \geq 5.3$ five times within a ninety-day interval. In fact, Norcia was among the locations that, apart from repeatedly experiencing strong ground motion, also hosted permanent instrumented stations and thus provided continuous accelerometric records throughout the sequence (as can be seen in Figure 2; see also, ReLUIS-INGV Workgroup, 2016; Luzi et al., 2017). Figure 8 shows two such cases as examples of the aforementioned situation, by providing pseudo-acceleration spectra of five ground motions recorded at the station of Amatrice (AMT) and another five recorded at one of the stations at Norcia (NRC) between August 24th and October 30th 2016 (EW component shown), details of the causal events can be found in Table 2. These records were selected on the basis that they exhibited the highest shaking intensities, primarily in terms of PGA but also considering spectral ordinates up to a period of 0.50s, recorded at those sites during the first ninety days of the sequence.

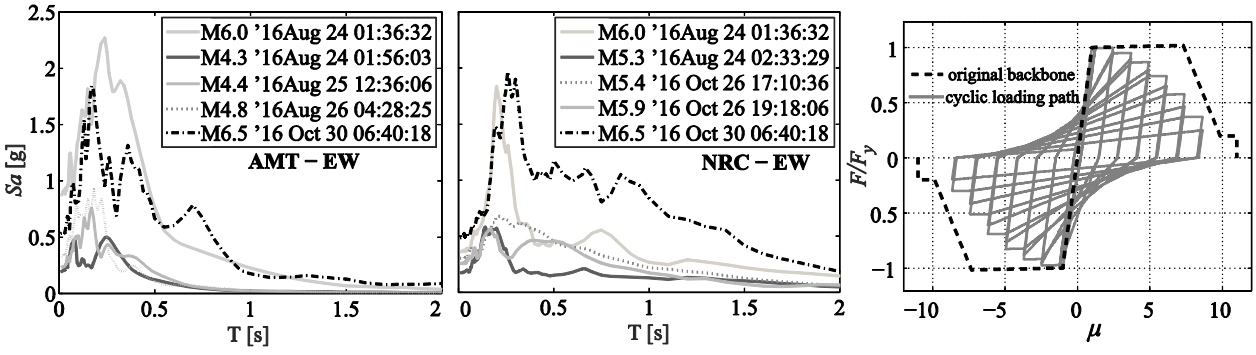

Figure 8. Pseudo-acceleration response spectra of the five shocks considered in the illustrative analysis of cumulative damage during the sequence at Amatrice (left) and Norcia (center). Backbone curve and cyclic loading hysteresis of the case-study SDOF systems (right).

Table 2. Event details corresponding to the response spectra shown in Figure 8.

Station	Date & Time (UTC)	ESM Event ID	M	Epi-central distance [km]	PGA EW [cm/s^2]	PGA NS [cm/s^2]
AMT	2016/08/24 01:36:32	EMSC-20160824_0000006	6.0	8.5	850.8	368.4
	2016/08/24 01:56:03	EMSC-20160824_0000007	4.3	3.6	190.4	152.7
	2016/08/25 12:36:06	EMSC-20160825_0000096	4.4	3.6	228.6	200.9
	2016/08/26 04:28:25	EMSC-20160826_0000013	4.8	3.1	318.7	329.8
	2016/10/30 06:40:18	EMSC-20161030_0000029	6.5	26.4	521.6	393.6
NRC	2016/08/24 01:36:32	EMSC-20160824_0000006	6.0	15.3	352.9	366.8
	2016/08/24 02:33:29	EMSC-20160824_0000013	5.3	4.4	167.0	190.8
	2016/10/26 17:10:36	EMSC-20161026_0000077	5.4	10.1	294.7	258.2
	2016/10/26 19:18:06	EMSC-20161026_0000095	5.9	13.2	248.3	366.4
	2016/10/30 06:40:18	EMSC-20161030_0000029	6.5	4.6	476.4	365.1

In this context of recurring shocks repeatedly producing high-to-moderate shaking intensity at certain sites within a relatively short span of time that practically precludes intermediate retrofit operations, emerges one of the principal features of the central Italy sequence; i.e., damage accumulation during a seismic sequence. Field reconnaissance missions undertaken shortly after the initiating M6.0 event of August 24th and also after the M6.5 shock of October 30th (e.g., GEER Workgroup, 2017) highlighted the fact that there were many structures left apparently undamaged (or only slightly damaged) after the initial event but were brought to a state of severe damage or near-collapse due to the cumulative degrading effect of the ensuing events. The phenomenon of damage accumulation during this sequence has been already touched upon by ReLUIS-INGV Workgroup (2016) and is showcased here as well.

In order to undertake an analytical study, illustrating the aforementioned issue of structural damage accumulation during the course of the sequence, a set of SDOF inelastic structures were considered. These structures follow the same peak-oriented hysteretic rule with moderate cyclic strength degradation as the one described in the preceding section, while the vibration period varies between 0.30 and 0.40s. Yield strength F_y is set to correspond to 20% of each structure's weight and the quadrilinear backbone (see Figure 8) is representative of the static pushovers of low-rise, low-code reinforced concrete buildings in central Italy.

The observation of the hysteretic response and evolution of a structural system throughout the sequence is used to provide some initial insights. Figure 9 shows the hysteretic response of two SDOF structures, one assumed at the AMT site and the other at NRC, during sequential dynamic excitation by the records whose spectra are shown in Figure 8. This response is then compared to that of the same system subjected to the October 30th M6.5 shock alone (on the left-hand side of the figure). At the end of each individual shock, the residual displacement is registered and plotted on the graphs and static pushover is carried out in both directions, providing the shape of the monotonic backbone's evolution during the sequence (*post-EQ* in the figure). Residual displacement is an engineering demand parameter that has seen extensive use as a proxy for the post-earthquake damage state of a building in seismic loss assessment (e.g., Ruiz-García and Miranda, 2006). The post-earthquake pushover on the other hand, offers additional information such as loss of stiffness (often termed period elongation) and loss of peak strength. Such information could be important when evolutionary hysteretic rules with strength degradation are considered, in merit of being more representative of the actual behavior of, among others, reinforced concrete structures (for a discussion of the effect of such hysteretic rules on residual displacements, see Liossatou and Fardis, 2015).

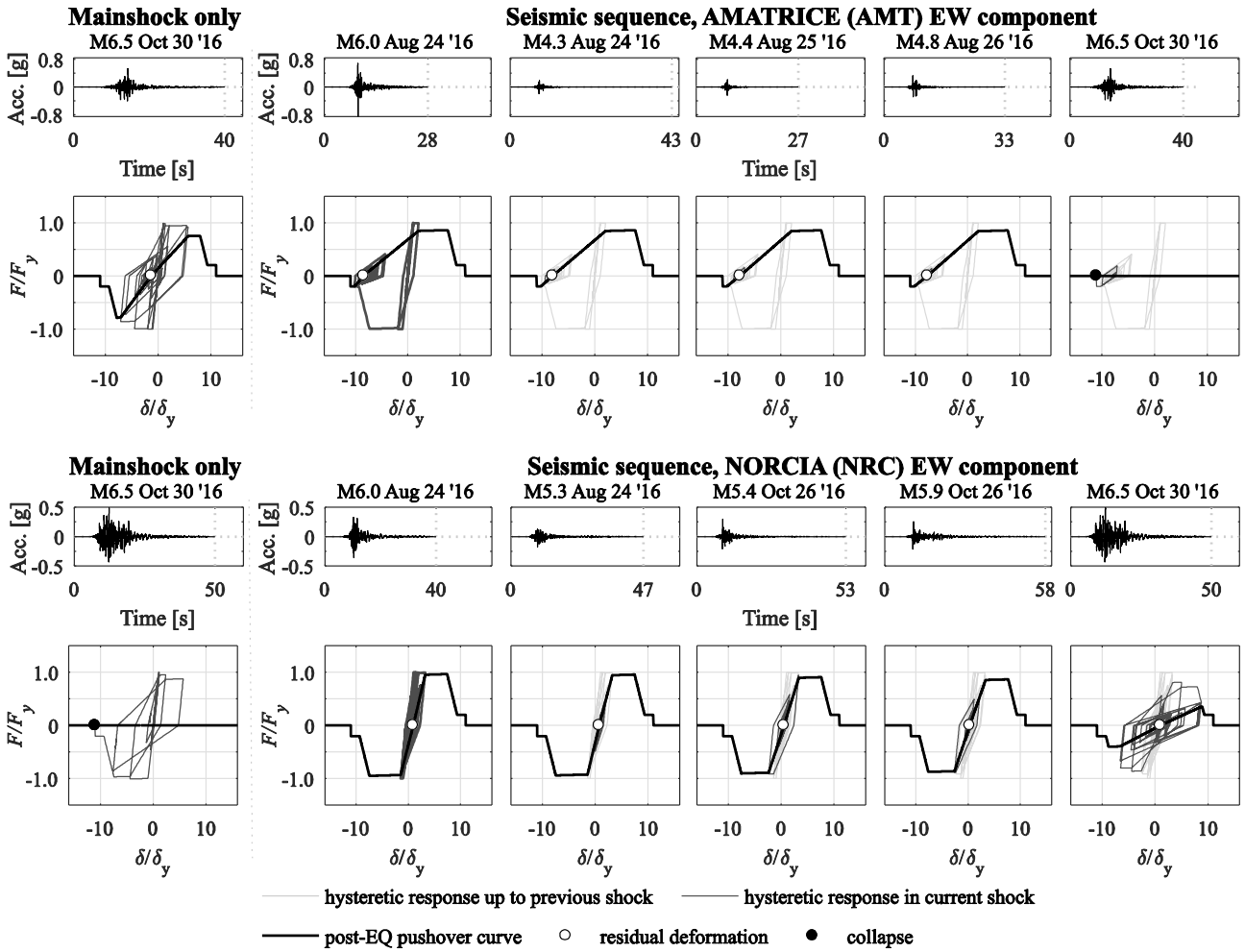

Figure 9. Hysteretic response and post-excitation static pushover considering single-shock versus sequential excitation for a $T = 0.30$s SDOF structure at AMT (top) and a $T = 0.40$s structure at NRC (bottom).

The upper panel of Figure 9 corresponds to a short-period structure assumed at the AMT site. Consideration of the October 30th M6.5 shock alone, leaves the structure still standing with some modest residual displacement but considerably damaged, as attested to by the loss of stiffness and peak strength apparent on the post-shock static pushover. Consideration of the entire sequence, however, tells a different story. The initial, pulse-like shock of the sequence leaves the structure severely damaged, with a large residual displacement apparently due to a single large inelastic excursion that brought the system into the in-cycle degradation domain of the descending branch of the backbone (for a discussion of cyclic versus in-cycle degradation, the interested reader is referred to FEMA-P440A, 2009). The next three shocks considered (low-magnitude shocks that occurred after the August 24th M6.0 event) make little impression on the damaged and reduced-stiffness system, producing modest ductility demands in the direction contrary to the residual displacement, where adequate residual strength still remains. It can be noted from Figure 8 and the response spectra of these three low-causal-magnitude shocks that, despite PGA values in the 0.20-0.30g range, the low-frequency content is too poor to cause significant inelastic demands, with Sa values rapidly dropping off after $T = 0.50s$. Then, the arrival of the fifth shock, which is in fact the mainshock of the sequence, predictably brings the damaged structure to almost immediate collapse during the very first inelastic excursion towards the direction of the residual drift.

The bottom panel of Figure 9 on the other hand, deals with a similar structure allegedly situated at the NRC site. In this case, direct application of the base acceleration produced by the October 30th M6.5 event to the undamaged model causes the hitherto intact structure to collapse after a number of ample inelastic cycles. During the first four shocks of the sequence considered, hysteresis is each time

characterized by only a few important cycles that leave the structure with a limited reduction in peak strength and mild period elongation. Residual displacement is not observed to increase monotonically and remains small. The mainshock leaves the structure severely damaged, but still standing, contrary to what was observed during its application onto the intact structure, which eventually collapsed. It is interesting to note that this behavior results from a complete reversal of the situation typically associated with a seismic sequence: instead of a large-amplitude shock followed by a series of less intense ground motions, the strongest shock in this case is preceded by the relatively weaker shocks of the sequence. Finally, it can be also observed that the severe loss of peak strength and significant period elongation resulting after the fifth consecutive shock, are not accompanied by a significant residual displacement; this situation is certainly reminiscent of the self-centering tendency of peak-oriented, degrading systems observed by Liossatou and Fardis (2015).

In overview, these two simple case-study examples highlighted some known issues, which may be far from novelties, but finding affirmation through a real sequence of numerous shocks of this intensity is in itself noteworthy. The first issue concerns the isolating effect of period elongation that can come with serious damage: while it may shield the affected structure from further damage due to low-magnitude shocks that lack significant spectral ordinates into the higher-period domain, a sequence of higher-magnitude shocks, with corresponding richer spectral shape, may prove to be not-as-forgiving. A second issue has to do with the tendency of some evolutionary hysteretic systems to exhibit low residual drifts during a multi-shock sequence, but accompanied by significant strength deterioration. The third issue emerges from the comparison of both example cases subjected to the entire sequence with the corresponding response to the mainshock alone: the comparison underlines that it is not only the shaking intensity of the individual shocks that determines the final damage state, but also the relative order of arrival, which can make the difference between collapse and survival of the structure; i.e., the so-called *sequence-effect*.

5. Conclusions

The present article discussed a variety of issues concerning seismic actions for seismic design and assessment, viewed through the lens of both structural engineering and engineering seismology. The discussion revolved around three main issues that emerged during the study and elaboration of near-source strong-motion accelerometric data collected during the 2016 central Italy seismic sequence. These issues are the probability of exceeding design seismic actions during major seismic events and the spatial disposition of the exceedance locations, near-source pulse-like seismic input, and the effect of a seismic sequence on structures expected to dissipate energy via inelastic deformation under a single strong earthquake event.

It was shown that due to the manner in which moderate-to-large magnitude events are accounted for in the definition of the code (uniform hazard) spectra in Italy, which is consistent with their probability of occurrence close to a specific site, when an earthquake with the same characteristics as the main events of the sequence occurs, the probability that said design actions will be exceeded in an area near to the source is high, possibly close to one. This result alone, which is confirmed by recorded ground motion in this and other recent Italian sequences, does not imply that hazard computations for the code spectrum underestimate the seismic threat for any specific site.

Pulse-like ground motions, identified among the near-source recordings obtained during the sequence, were studied from a structural engineering point of view. The anticipated systematic difference, in terms of average spectral shape, between this type of seismic input and non-impulsive (ordinary) strong motion was discussed. The well-known effect of pulse duration on the seismic demand imposed by impulsive records to inelastic structures was showcased also with respect to existing predictive models. The investigation of this sequence confirmed the relevance of near-source

directivity pulses with respect to structural response in seismic areas with prevalent normal focal mechanisms, such as those found along the Apennine mountain chain.

Finally, this article sought to take advantage of those accelerometric stations that recorded multiple instances of strong motion during the first ninety days of the sequence, to present a number of case-studies that offered interesting insights into the topic of damage accumulation in structures. Although research into seismic damage is typically placed within the context of purely mainshock-followed-by-aftershock sequences, the central Italy sequence includes multiple moderate-to-high magnitude events in close temporal succession, that may be more relevant in that respect. Case-study examples specific to this sequence, confirmed that low-magnitude events occurring during the sequence at very close distances to an already-damaged structure may exhibit large amplitudes in the high-frequency range, but may lack the low-frequency richness and corresponding spectral shape to cause significant inelastic displacement demands and hence damage accumulation. On the other hand, this sequence was observed to have had the potential for more severe damage accumulation phenomena, by virtue of the several moderate-to-high magnitude events comprising it. This was mainly due to ground motions recorded at specific sites that repeatedly found themselves in near-source conditions during these main seismic events. Another noteworthy affirmation of a known effect was that, when structural dynamic response is characterized by stiffness and strength degradation of the constituent materials, the evolutionary nature of hysteretic behavior could in effect isolate a structure from further damage in subsequent shocks. Finally, as expected for evolutionary hysteretic behavior, the sequence effect is not additive; i.e., given the individual ground motions, their order of arrival determines the structural damage progression.

Acknowledgements

The study presented in this paper was developed within the activities of ReLUIS *(Rete dei Laboratori Universitari di Ingegneria Sismica)* for the project ReLUIS-DPC 2014- 2018, as well as within the H2020-MSCA-RISE-2015 research project EXCHANGE-Risk (grant agreement number 691213).

References

Akinci A, Malagnini L, Sabetta F (2010) Characteristics of the strong ground motions from the 6 April 2009 L'Aquila earthquake, Italy. Soil Dyn Earthq Eng 30:320-335

Altoonash A, Deierlein G (2004) Simulation and damage models for performance assessment of reinforced concrete beam-column joints, Ph.D. Dissertation, Stanford University.

Ambraseys NN, Simpson KA, Bommer JJ (1996) Prediction of horizontal response spectra in Europe. Earthq Eng Struct D 25:371–400

Baker JW (2007) Quantitative Classification of Near-Fault Ground Motions Using Wavelet Analysis. Bull Seism Soc Am 97(5):1486–1501

Baker JW, Cornell CA (2005) A vector-valued ground motion intensity measure consisting of spectral acceleration and epsilon. Earthq Eng Struct D 34(10):1193-1217

Baltzopoulos G, Vamvatsikos D, Iervolino I (2016) Analytical modelling of near-source pulse-like seismic demand for multi-linear backbone oscillators. Earthq Eng Struct D 45(11):1797–1815

Bertero V, Mahin S, Herrera R (1978) Aseismic design implications of near-fault San Fernando earthquake records. Earthq Eng Struct D 6(1):31–42

Bojórquez E, Iervolino I (2011) Spectral shape proxies and nonlinear structural response, Soil Dyn Earthq Eng 31(7):996-1008

Bommer JJ, Douglas J, Strasser FO (2003) Style-of-faulting in ground-motion prediction equations. Bull Earthq Eng 1:171-203

Chioccarelli E, Iervolino I (2010) Near-Source Seismic Demand and Pulse-Like Records: a Discussion for L'Aquila Earthquake. Earthq Eng Struct D 39(9):1039–1062

CS.LL.PP. (2008) Decreto Ministeriale 14 gennaio 2008: Norme tecniche per le costruzioni. Gazzetta Ufficiale della Repubblica Italiana, 29 (in Italian)

FEMA P440A (2009) Effects of Strength and Stiffness Degradation on Seismic Response. Prepared by ATC for FEMA, Redwood City, California

GEER Workgroup (2017) Engineering Reconnaissance Following the October 2016 Central Italy Earthquakes - Version 2 Report number: GEER-050D DOI: 10.18118/G6HS39

Howard JK, Tracy CA, Burns RG (2005) Comparing observed and predicted directivity in near-source ground motion. Earthq Spectra 21(4):1063–1092

Iervolino I (2013) Probabilities and fallacies: why hazard maps cannot be validated by individual earthquakes. Earthq Spectra 29(3):125–1136

Iervolino I, Baltzopoulos G, Chioccarelli E (2016a) Preliminary engineering analysis of the August 24th, M_L6.0 central Italy earthquake records. Ann Geophys-Italy 59(fast track 5) DOI: 10.4401/ag-7182

Iervolino I, Chioccarelli E, Baltzopoulos G (2012a) Inelastic displacement ratio of near-source pulse-like ground motions. Earthquake Eng Struct Dyn 41:2351–2357

Iervolino I, Chioccarelli E, Convertito V (2011) Engineering design earthquakes from multimodal hazard disaggregation. Soil Dyn Earthq Eng 31:1212-1231

Iervolino I, Cornell CA (2008) Probability of occurrence of velocity pulses in near-source ground motions. Bull Seismol Soc Am 98(5):2262-2277

Iervolino I, De Luca F, Chioccarelli E (2012b) Engineering seismic demand in the 2012 Emilia sequence: preliminary analysis and model compatibility assessment. Ann Geophys-Italy 55:4: 639-645

Iervolino I, Giorgio M, Chioccarelli E (2016b). Markovian modeling of seismic damage accumulation. Earthq Eng Struct D 45(3):441-461

INGV Seismological Data Centre (1997) Rete Sismica Nazionale (RSN). Istituto Nazionale di Geofisica e Vulcanologia (INGV) Italy. https://doi.org/10.13127/SD/X0FXnH7QfY

Joyner WB, Boore DM (1981) Peak horizontal acceleration and velocity from strongmotion records including records from the 1979 Imperial Valley, California, Earthquake. Bull Seismol Soc Am 71:2011–2038

Liossatou E, Fardis MN (2015). Residual displacements of RC structures as SDOF systems. Earthquake Engng Struct Dyn 44:713–734

Luzi L, Pacor F, Puglia R, Lanzano G, Felicetta C, D'amico M, Michelini A, Faenza L, Lauciani V, Iervolino I, Baltzopoulos G, Chioccarelli E (2017) The Central Italy seismic sequence between August and December 2016: analysis of strong-motion observations. Seismol Res Lett (in press)

McGuire RK (2004) Seismic hazard and risk analysis. Report MNO-10. Oakland, CA, USA: Earthquake Engineering Research Institute Publication

Meletti C, D'Amico V, Ameri G, Rovida A, Stucchi M (2012) Seismic hazard in the Po plain and the 2012 Emilia earthquakes. Ann Geophys-Italy 55(4):623-629

Meletti C, Galadini F, Valensise G, Stucchi M, Basili R, Barba S, Vannucci G, Boschi E (2008) A seismic source zone model for the seismic hazard assessment of the Italian territory. Tectonophysics 450(1):85–108

Monaco P, Totani G, Barla G, Cavallaro A, Costanzo A, D'Onofrio A, Evangelista L, et al. (2009) Geotechnical aspects of the L'Aquila earthquake, proceedings of the Earthquake Geotechnical Engineering Satellite Conference, XVIIth International Conference on Soil Mechanics and Geotechnical Engineering, Alexandria, Egypt

Poiata N, Miyake H, Koketsu K (2017) Mechanisms for generation of near-fault ground motion pulses for dip-slip faulting. Pure Appl Geophys DOI 10.1007/s00024-017-1540-z

Presidency of Council of Ministers - Civil Protection Department (1972). Italian Strong Motion Network. Presidency of Council of Ministers - Civil Protection Department. Other/Seismic Network. doi:10.7914/SN/IT

ReLUIS-INGV Workgroup (2016) Preliminary study on strong motion data of the 2016 central Italy seismic sequence V6, available at http://www.reluis.it

Ruiz-García J, Miranda E (2006) Evaluation of residual drift demands in regular multi-storey frames for performance-based seismic assessment. Earthq Eng Struct D 35:1609–1629

Shahi S, Baker JW (2011) An empirically calibrated framework for including the effects of near-fault directivity in probabilistic seismic hazard analysis. Bull Seismol Soc Am 101(2):742-755

Somerville PG, Smith NF, Graves RW, Abrahamson NA (1997) Modification of empirical strong ground motion attenuation relations to include the amplitude and duration effects of rupture directivity. Seismol Res Lett 68:199–222

Stucchi M, Meletti C, Montaldo V, Crowley H, Calvi GM, Boschi E (2011) Seismic hazard assessment (2003–2009) for the Italian Building Code. Bull Seismol Soc Am 101(4):1885-1911

Tothong P, Cornell CA (2008) Structural performance assessment under near-source pulse-like ground motions using advanced ground motion intensity measures. Earthq Eng Struct D 37(7):1013-1037

Vamvatsikos D, Cornell CA (2002) Incremental dynamic analysis. Earthq Eng Struct D 31:491-514

Vamvatsikos D, Cornell CA (2005) Direct estimation of seismic demand and capacity of multiple-degree-of-freedom systems through incremental dynamic analysis of single degree of freedom approximation. J Struct Eng 31:589-599

Yeo GL, Cornell CA (2009) Building life-cycle cost analysis due to mainshock and aftershock occurrence. Struct Saf 31:396-408